Combustion Theory and Modelling
Publication details, including instructions for authors and subscription information:
http://www.tandfonline.com/loi/tctm20

Effects of heat conduction and radical quenching on premixed stagnation flame stabilised by a wall

Huangwei Zhang [a] & Zheng Chen [b]

[a] Department of Engineering, University of Cambridge , UK

[b] State Key Laboratory for Turbulence and Complex Systems, Department of Mechanics and Aerospace Engineering, College of Engineering, Peking University , Beijing , 100871 , China

Published online: 14 Jun 2013.

To cite this article: Huangwei Zhang & Zheng Chen (2013): Effects of heat conduction and radical quenching on premixed stagnation flame stabilised by a wall, Combustion Theory and Modelling, DOI:10.1080/13647830.2013.792393

To link to this article: http://dx.doi.org/10.1080/13647830.2013.792393

Combustion Theory and Modelling, 2013
http://dx.doi.org/10.1080/13647830.2013.792393

Taylor & Francis
Taylor & Francis Group

Effects of heat conduction and radical quenching on premixed stagnation flame stabilised by a wall

Huangwei Zhang[a*] and Zheng Chen[b]

[a]*Department of Engineering, University of Cambridge, UK;* [b]*State Key Laboratory for Turbulence and Complex Systems, Department of Mechanics and Aerospace Engineering, College of Engineering, Peking University, Beijing 100871, China*

(*Received 3 November 2012; revised 7 March 2013; final version received 18 March 2013*)

The premixed stagnation flame stabilised by a wall is analysed theoretically considering thermally sensitive intermediate kinetics. We consider the limit case of infinitely large activation energy of the chain-branching reaction, in which the radical is produced infinitely fast once the cross-over temperature is reached. Under the assumptions of potential flow field and constant density, the correlation for flame position and stretch rate of the premixed stagnation flame is derived. Based on this correlation, the effects of heat conduction and radical quenching on the wall surface are examined. The wall temperature is shown to have great impact on flame bifurcation and extinction, especially when the flame is close to the wall. Different flame structures are observed for near-wall normal flame, weak flame, and critically quenched flame. The fuel and radical Lewis numbers are found to have opposite effects on the extinction stretch rate. Moreover, it is also demonstrated that only when the flame is close to the wall does the radical quenching strongly influence the flame bifurcation and extinction. The extinction stretch rate is shown to decrease with the amount of radical quenching for different fuel and radical Lewis numbers. Besides, the coupling between the wall heat conduction and radical quenching is found to greatly influence the bifurcation and extinction of the premixed stagnation flame.

Keywords: flame-wall interaction; premixed stagnation flame; extinction stretch rate; heat conduction; radical quenching

1. Introduction

Flame-wall interaction is the phenomenon in which premixed flames and wall surfaces affect each other through the coupling of chemistry, momentum, and energy [1]. It can be commonly found in laboratory burners as well as industrial combustion systems such as gas turbine combustors and furnaces. Recently, development of novel combustion technologies such as meso- and micro-scale combustion devices, catalytic fuel synthesis, and low-emission burners has stimulated the interests to understand the flame-wall interaction [2–4]. However, since different processes such as flame extinction, stabilisation, bifurcations, and radical quenching are involved in the flame-wall interaction, the underlying mechanisms for flame-wall interaction are still not well understood.

In the literature, there are many studies on the flame-wall interaction. The early effort on this topic was motivated by understanding the quenching distance and therein exhaust emissions in practical combustion devices such as engines and gas turbines [5–7]. Later, Westbrook *et al*. [8] numerically studied flame quenching near an inert wall with detailed

*Corresponding author. Email: hz283@cam.ac.uk

chemistry and found that the temperature dependence of chaining-branching and radical recombination reactions was responsible for flame extinguishment near the wall. Using a two-step chemistry model, Hocks *et al*. [9] theoretically examined the influence of chain-branching and chain recombination reaction rates on the transient flame quenching near a cold wall. Vlachos *et al*. [10] analysed the bifurcations of a homogeneous hydrogen flame near an inert wall and identified the dominant species for ignition and extinction. Egolfopoulos *et al*. [11] investigated the extinction and propagation of both single jet-wall and opposed jet flames and discussed the relations between wall temperature and extinction strain rate as well as laminar flame speed. Ju and Minaev [12] studied the effects of a hot wall on the lean flammability limits and flame bifurcations. Nakamura *et al*. [13] found that the wall temperature has a dominant influence on repetitive ignition and extinction of premixed flames in a micro-flow reactor. Some studies on the wall heat flux when the flame approaches a cold wall were reported [14–18]. These aforementioned investigators discussed the behaviours of the premixed flame stabilised by a wall from different aspects. However, the influence of wall temperature and Lewis numbers on the extinction and bifurcations of a wall-stabilised premixed flame is still not clear.

The radical quenching near a wall has also been investigated in the literature. Egolfopoulos *et al.* [11] studied the effect of H radical recombination at the wall on the extinction stretch rate and found that this effect is important for high wall temperature. Surface radical recombination reactions on the chemically reactive or catalytic wall were considered for premixed hydrogen/air flames and the impact of wall quenching of radicals on ignition, extinction and stabilisation of premixed flames was analysed [19–22]. The concentration of OH radical in the chemical quenching of methane/air premixed flames in a narrow channel with different wall materials was investigated experimentally and numerically and the results showed that the different wall materials lead to the different extent of radical quenching [23]. It is well known that radical quenching on a wall is a highly coupled physical and chemical process and lots of factors such as radical transport ability and wall materials are involved [2, 3]. The above investigations are limited to one specific fuel and wall material and thereby it is still difficult to generalise the findings therein. In order to gain a clear understanding of radical quenching, it is necessary to conduct theoretical analysis on the influence of radical quenching on premixed flames close to a chemically reactive wall surface.

The objective of this study is to theoretically investigate the effects of wall heat conduction and radical quenching on premixed stagnation flame stabilised by a wall. In the following, the mathematical model and theoretical analysis are presented in Section 2 and Section 3, respectively. In Section 4, the effects of wall heat conduction and radical quenching on stretched premixed flames are discussed. Finally, the conclusions are presented in Section 5.

2. Mathematical model

The simplified Zel'dovich-Liñán model proposed by Dold and co-workers [24, 25] is employed in the present analysis. This model consists of a chain-branching reaction $F + Z \rightarrow 2Z$ and a recombination reaction $Z + M \rightarrow P + M$, where F, Z, and P denote fuel, radical, and product, respectively, and M represents any third body species. The chain-branching reaction is assumed to have high activation energy but is thermally neutral, while the recombination reaction is assumed to be temperature insensitive but releases all the heat [25]. This model was used in previous studies on the ignition, propagation, extinction, and stability of premixed flames [24–35].

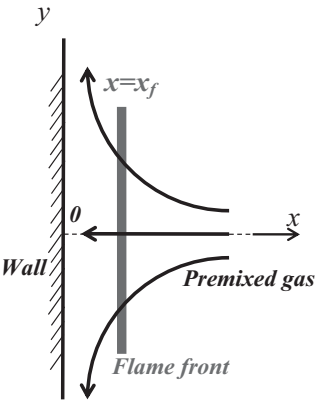

Figure 1. The schematic diagram of premixed stagnation flame stabilised by a wall.

Figure 1 shows the schematic diagram of the premixed stagnation flame stabilised by a wall, which is the fundamental flame configuration of flame-wall interaction and hence is considered in this study. The fresh pre-mixture is perpendicularly impinged to an impermeable head-on wall whose temperature is fixed to be some constant value. The potential flow assumption is employed and the velocity in the axial direction (perpendicular to the stagnation surface) is $\tilde{u} = -\tilde{k}\tilde{x}$, where $\tilde{k}$ is the strain rate (also referred to as stretch rate). For the one-dimensional stagnation flame, the governing equations for the mass fractions of fuel, $\tilde{Y}_F$, and radical, $\tilde{Y}_Z$, and temperature, $\tilde{T}$, are

$$-\tilde{\rho}\tilde{k}\tilde{x}\frac{d\tilde{Y}_F}{d\tilde{x}} = \frac{d}{d\tilde{x}}\left(\tilde{\rho}\tilde{D}_F\frac{d\tilde{Y}_F}{d\tilde{x}}\right) - \tilde{W}_F\tilde{\omega}_B \tag{1a}$$

$$-\tilde{\rho}\tilde{k}\tilde{x}\frac{d\tilde{Y}_Z}{d\tilde{x}} = \frac{d}{d\tilde{x}}\left(\tilde{\rho}\tilde{D}_Z\frac{d\tilde{Y}_Z}{d\tilde{x}}\right) + \tilde{W}_Z\left(\tilde{\omega}_B - \tilde{\omega}_C\right) \tag{1b}$$

$$-\tilde{\rho}\tilde{C}_P\tilde{k}\tilde{x}\frac{d\tilde{T}}{d\tilde{x}} = \frac{d}{d\tilde{x}}\left(\tilde{\lambda}\frac{d\tilde{T}}{d\tilde{x}}\right) + \tilde{Q}\tilde{\omega}_C \tag{1c}$$

The density $\tilde{\rho}$, specific heat capacity $\tilde{C}_P$, fuel mass diffusivity $\tilde{D}_F$, radical mass diffusivity $\tilde{D}_Z$, and thermal conductivity $\tilde{\lambda}$ are all assumed to be constant. The variable $\tilde{Q}$ denotes the heat release of the recombination reaction. The reaction rates of the chain-branching and recombination reactions take the following form [25, 35]

$$\tilde{\omega}_B = \frac{\tilde{\rho}\tilde{Y}_F}{\tilde{W}_F}\frac{\tilde{\rho}\tilde{Y}_Z}{\tilde{W}_Z}\tilde{A}_B\exp\left(-\frac{\tilde{T}_B}{\tilde{T}}\right),\ \tilde{\omega}_C = \frac{\tilde{\rho}\tilde{Y}_Z}{\tilde{W}_Z}\frac{\tilde{\rho}}{\tilde{W}}\tilde{A}_C \tag{2a, b}$$

where $\tilde{W}_F$ and $\tilde{W}_Z$ are the molecular weights of fuel and radical, respectively, $\tilde{W}$ the mean molecular weight, $\tilde{A}_B$ and $\tilde{A}_C$ the frequency factors of the chain-branching and recombination reactions, respectively, and $\tilde{T}_B$ the activation temperature of the chain-branching reaction.

We introduce the following non-dimensional variables

$$x = \frac{\tilde{x}}{\tilde{x}_s}, \quad T = \frac{\tilde{T} - \tilde{T}_0}{\tilde{T}_s}, \quad Y_F = \frac{\tilde{Y}_F}{\tilde{Y}_{F0}}, \quad Y_Z = \frac{\tilde{Y}_Z}{\tilde{Y}_{Zs}}, \quad k = \tilde{t}_s \tilde{k} \tag{3}$$

along with the definitions

$$\tilde{t}_s = \frac{\tilde{x}_s^2 \tilde{\rho} \tilde{C}_P}{\tilde{\lambda}}, \quad \tilde{x}_s^2 = \frac{\tilde{\lambda} \tilde{W}}{\tilde{\rho}^2 \tilde{C}_P \tilde{A}_C}, \quad \tilde{Y}_{Zs} = \frac{\tilde{W}_Z \tilde{Y}_{F0}}{\tilde{W}_F},$$
$$Q = \frac{\tilde{Q} \tilde{Y}_{F0}}{\tilde{C}_P \tilde{T}_s \tilde{W}_F}, \quad \beta = \frac{\tilde{T}_B \tilde{T}_s}{(\tilde{T}_0 + \tilde{T}_s)^2}, \quad \sigma = \frac{\tilde{T}_s}{\tilde{T}_0 + \tilde{T}_s} \tag{4}$$

where $\tilde{T}_0$ and $\tilde{Y}_{F0}$ are the temperature and fuel mass fraction in the fresh mixture, respectively. The Zel'dovich number, β, and the scaling temperature, $\tilde{T}_s$, can be determined by the requirement that the equality $\tilde{\omega}_B = \beta^2 \tilde{\omega}_C$ holds at the temperature of $\tilde{T}_0 + \tilde{T}_s$ [25].

Substituting Equations (3) and (4) into (1) yields the following non-dimensional governing equations

$$-kx \frac{dY_F}{dx} = \frac{1}{Le_F} \frac{d^2 Y_F}{dx^2} - \omega \tag{5a}$$

$$-kx \frac{dY_Z}{dx} = \frac{1}{Le_Z} \frac{d^2 Y_Z}{dx^2} - Y_Z + \omega \tag{5b}$$

$$-kx \frac{dT}{dx} = \frac{d^2 T}{dx^2} + Q Y_Z \tag{5c}$$

where $Le_F = \lambda/(\rho C_P D_F)$ and $Le_Z = \lambda/(\rho C_P D_Z)$ are the Lewis numbers of fuel F and radical Z, respectively. The normalised reaction rate ω in Equations (5a) and (5b) is

$$\omega = \beta^2 Y_F Y_Z \exp\left[\beta \frac{T - 1}{1 + \sigma(T - 1)}\right] \tag{6}$$

The non-dimensional boundary conditions at the wall surface ($x = 0$) and upstream fresh pre-mixture ($x \to +\infty$) are

$$x = 0: \quad T = T_w, \quad \frac{dY_F}{dx} = 0, \quad \frac{dY_Z}{dx} = -r_q Y_Z \tag{7a}$$

$$x \to \infty: \quad T = 0, \quad Y_F = 1, \quad Y_Z = 0 \tag{7b}$$

with T_w being the normalised wall temperature. The radical quenching due to the non-inert wall is mimicked by the radical sink on the wall in the third equality of Equation (7a), in which r_q is the wall's radical quenching coefficient determined by the properties of the wall surface and the mass diffusivity and reactivity of the radical [2–4]. The coefficient r_q is negative when the radical is quenched/destructed on the wall surface.

In the limit of large activation energy ($\beta \to +\infty$), the thermally sensitive chain-branching reaction is confined at an infinitesimally thin flame sheet which is located at $x = x_f$ (i.e. x_f is the distance between the flame sheet and wall surface as shown in Figure 1). For more details concerning the assumption of large activation energy, one can refer to the pioneering work by Liñán [36]. According to the asymptotic analysis conducted by Dold and co-workers [24, 25, 35], the following conditions must hold across or at the flame front ($x = x_f$)

$$[Y_F] = [Y_Z] = [T] = T - 1 = \left[\frac{dT}{dx}\right] = \left[\frac{1}{Le_F}\frac{dY_F}{dx} + \frac{1}{Le_Z}\frac{dY_Z}{dx}\right] = Y_F\frac{dT}{dx} = 0 \qquad (8)$$

where the square brackets denote the difference between the variables on the unburned and burned sides, i.e. $[f] = f\left(x = x_f^+\right) - f\left(x = x_f^-\right)$. Under the assumption of large activation energy, the dimensionless temperature at the flame front is $T_f = 1$, which is approximately equal to the crossover temperature T_c in the leading-order analysis [35].

3. Theoretical analysis

The rate of the chain-branching reaction, ω, can be neglected in both the unburned ($x_f \le x \le +\infty$) and burned ($0 \le x \le x_f$) zones when the chain-branching reaction zone is infinitesimally thin in the limit of large activation energy. Consequently, with the boundary conditions (7a, 7b) and jump conditions (8), Equations (5a)–(5c) with zero reaction rate ($\omega = 0$) can be solved analytically in the unburned and burned zones. The fuel mass fraction in the burned zone is zero according to the fuel lean assumption and that in the unburned zone is obtained by solving Equation (5b) together with the conditions in Equations (7b) and (8), which gives

$$Y_F(x) = \begin{cases} 0 & if \quad 0 \le x \le x_f \\ \dfrac{\mathrm{erf}(\sqrt{Le_F k/2}x) - \mathrm{erf}(\sqrt{Le_F k/2}x_f)}{1 - \mathrm{erf}(\sqrt{Le_F k/2}x_f)} & if \quad x_f \le x \le +\infty \end{cases} \qquad (9)$$

where $\mathrm{erf}(\tau) = 2/\sqrt{\pi} \cdot \int_0^\tau e^{-\varsigma^2} d\varsigma$ is the error function.

The solution for the radical mass fraction $Y_Z(x)$ is

$$Y_Z(x) = \begin{cases} Y_{Zf} e^{\frac{1}{2}Le_Z k(x_f^2 - x^2)}\left[\dfrac{J^-(1/k, \sqrt{Le_Z k/2}x)}{\phi^-} + \dfrac{J^+(1/k, \sqrt{Le_Z k/2}x)}{\phi^+}\right] & if\ 0 \le x \le x_f \\ Y_{Zf} e^{\frac{1}{2}Le_Z k(x_f^2 - x^2)} \dfrac{J^-(1/k, \sqrt{Le_Z k/2}x)}{J^-(1/k, \sqrt{Le_Z k/2}x_f)} & if\ x_f \le x \le +\infty \end{cases} \qquad (10)$$

where

$$J^{\pm}(a,b)=\int_0^{\infty}\varsigma^a\exp(-\varsigma^2/4\pm b\varsigma)d\varsigma \tag{11a}$$

$$\phi^{\pm}=J^{\pm}(1/k,\sqrt{Le_Zk/2}x_f)-(\vartheta^{\pm}/\vartheta^{\mp})J^{\mp}(1/k,\sqrt{Le_Zk/2}x_f) \tag{11b}$$

$$\vartheta^{\pm}=\pm\sqrt{Le_Zk/2}\cdot J^{\pm}(1+1/k,0)+r_q\cdot J^{\pm}(1/k,0) \tag{11c}$$

At the limit of $r_q\to-\infty$, which corresponds to the complete radical destruction at the wall (i.e. $Y_Z=0$ at $x_f=0$), we have $\vartheta^{\pm}/\vartheta^{\mp}\to 1.0$ and hence Equation (11b) is reduced to

$$\phi^{\pm}=J^{\pm}(1/k,\sqrt{Le_Zk/2}x_f)-J^{\mp}(1/k,\sqrt{Le_Zk/2}x_f) \tag{12}$$

Substituting Equation (12) into Equation (10) yields the following expression for the radical mass fraction in the burned zone ($0\le x\le x_f$)

$$Y_Z(x)=Y_{Zf}e^{\frac{1}{2}Le_Zk(x_f^2-x^2)}\frac{J^{-}(1k,\sqrt{Le_Zk/2}x)-J^{+}(1/k,\sqrt{Le_Zk/2}x)}{J^{-}(1/k,\sqrt{Le_Zk/2}x_f)-J^{+}(1/k,\sqrt{Le_Zk/2}x_f)} \tag{13}$$

which can also be solved using the equivalent boundary condition $Y_Z=0$ at $x_f=0$.

In Equations (10) and (13), Y_{Zf} is the radical mass fraction at the flame front, i.e. $Y_Z(x=x_f)=Y_{Zf}$. According to the requirement of $[Le_F{}^{-1}dY_F/dx+Le_Z{}^{-1}dY_Z/dx]=0$ at $x=x_f$ in Equation (8), we have

$$Y_{Zf}=\frac{\sqrt{2Le_Z/k}e^{-\frac{1}{2}Le_Fkx_f^2}}{Le_F\Theta(k,x_f)\int_{x_f}^{\infty}e^{-\frac{1}{2}Le_Fk\tau^2}d\tau} \tag{14}$$

in which

$$\begin{aligned}\Theta(k,x_f)=&\left[-\frac{J^{-}(1+1/k,\sqrt{Le_Zk/2}x_f)}{\phi^{-}}+\frac{J^{+}(1+1/k,\sqrt{Le_Zk/2}x_f)}{\phi^{+}}\right]\\&+\frac{J^{-}(1+1/k,\sqrt{Le_Zk/2}x_f)}{J^{-}(1/k,\sqrt{Le_Zk/2}x_f)}-\sqrt{2Le_Zk}x_f\\&\times\left[\frac{J^{-}(1/k,\sqrt{Le_Zk/2}x_f)}{\phi^{-}}+\frac{J^{+}(1/k,\sqrt{Le_Zk/2}x_f)}{\phi^{+}}\right]+\sqrt{2Le_Zk}x_f\end{aligned} \tag{15}$$

Using the condition of $T(x=x_f)=1$ in Equation (8) and the boundary conditions in Equation (7), the analytical solution for the temperature distribution can be obtained

as

$$T(x) = \begin{cases} \frac{\int_x^{x_f} e^{-\frac{1}{2}\varsigma^2 k} d\varsigma}{\int_0^{x_f} e^{-\frac{1}{2}\varsigma^2 k} d\varsigma} \left[T_w - 1 + \int_0^{x_f} \int_\eta^\infty I(\varsigma, \eta) d\varsigma d\eta \right] - \int_x^{x_f} \int_\eta^\infty I(\varsigma, \eta) d\varsigma d\eta + 1 & \text{if } 0 \le x \le x_f \\ \frac{\int_x^\infty e^{-\frac{1}{2}\varsigma^2 k} d\varsigma}{\int_{x_f}^\infty e^{-\frac{1}{2}\varsigma^2 k} d\varsigma} \left[1 + \int_{x_f}^\infty \int_\eta^\infty I(\varsigma, \eta) d\varsigma d\eta \right] - \int_x^\infty \int_\eta^\infty I(\varsigma, \eta) d\varsigma d\eta & \text{if } x_f \le x \le +\infty \end{cases} \tag{16}$$

in which $I(\varsigma, \eta) = QY_z(\varsigma) e^{\frac{1}{2}k(\varsigma^2 - \eta^2)}$.

Substituting the above temperature distribution into the requirement of heat flux continuity ($[dT/dx] = 0$ at $x = x_f$ in Equation (8)) yields the following algebraic relationship between the stretch rate k and flame position x_f

$$\int_0^{x_f} e^{-\frac{1}{2}\varsigma^2 k} d\varsigma \left[1 + \int_{x_f}^\infty \int_\eta^\infty I(\varsigma, \eta) d\varsigma d\eta \right] = \int_{x_f}^\infty e^{-\frac{1}{2}\varsigma^2 k} d\varsigma \left[T_w - 1 + \int_0^{x_f} \int_\eta^\infty I(\varsigma, \eta) d\varsigma d\eta \right] \tag{17}$$

which includes fuel and radical Lewis numbers (Le_F and Le_Z), heat release (Q), wall temperature (T_w) and radical quenching coefficient (r_q). By numerically solving Equation (17), we can get the flame position (x_f) at different values of stretch rate (k). The effects of heat conduction to/from and radical quenching on the wall can be assessed by changing the values of T_w and r_q, respectively. Moreover, the effects of fuel Lewis number (Le_F) and radical Lewis number (Le_Z) can also be examined.

For comparison, we also consider the premixed stagnation flame stabilised by an adiabatic wall (i.e. $dT/dx|_{x=0} = 0$). Following the similar mathematical derivations, we obtain the relationship describing the stretch rate k and flame position x_f as

$$\int_{x_f}^\infty \int_0^\eta I(\varsigma, \eta) d\varsigma d\eta = 1 \tag{18}$$

Equation (18) implicitly includes fuel and radical Lewis numbers (Le_F and Le_Z) and heat release (Q). In this study, the effects of heat release are not considered and therefore the non-dimensional heat release is fixed to be $Q = 2.0$, a value that corresponds to a typical hydrocarbon mixture with initial temperature at 300∼500 K [25].

4. Results and discussion

4.1. *Effects of wall temperature*

With the help of Equation (17), the effects of wall temperature and hence wall heat conduction on the premixed stagnation flame stabilised by a chemically inert wall (i.e. without radical quenching, $r_q = 0$) are investigated in this subsection. For unit fuel and radical Lewis number ($Le_F = Le_Z = 1$), the change of the flame position with the stretch rate at different wall temperatures is plotted in Figure 2. It is seen when the wall temperature is below the cross-over temperature ($T_w < T_c = T_f = 1.0$), there are dual solutions of flame position x_f for relatively small stretch rate k. The premixed stagnation flame approaches the

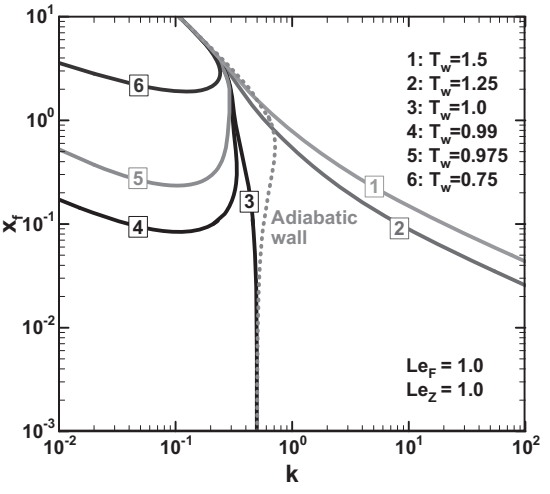

Figure 2. Flame position as a function of stretch rate at different wall temperatures.

wall as the stretch rate increases, and flame extinction occurs at the turning point beyond which no stagnation flame can exist. The stretch rate at the turning point is referred to as the extinction stretch rate and it is denoted by k_{ext}. It is noted that the effects of radiation are not considered in the present study and the turning point corresponds to the so-called stretch-induced extinction, which is also observed in counterflow, stagnation, and tubular flames [37–40]. When $T_w = T_c = 1$, we have $x_f \to 0$ for $k \to 0.5$, indicating that the premixed stagnation flame can exist until it touches the wall surface. When the wall temperature is above the cross-over temperature ($T_w > T_c = 1.0$), Figure 2 shows that the flame front can consecutively approach the wall and no flame extinguishment can be observed. This is because the radical can always be produced through the chain-branching reaction when the local temperature is above the cross-over temperature. Therefore, as indicated by Figure 2, the wall temperature has a pronounced effect on bifurcations and extinguishment of the premixed stagnation flame. Moreover, as a comparison, the results obtained from Equation (18) for the case of the adiabatic wall are also plotted in Figure 2 (dashed line). The comparison indicates that extinction is prompted/inhibited when the wall temperature is below/above the cross-over temperature.

Figure 3 shows the flame structures at different stretch rates for $T_w = 1.25$ and $Le_F = Le_Z = 1$. At a low stretch rate of $k = 0.1$, the flame is far away from the wall ($x_f = 10.75$). For this case, the maximum temperature is close to the normalised adiabatic flame temperature, $T_{ad} \approx 2.0$ (in the present chemical model, $T_{ad} \approx Q$, which can be derived from the one-dimensional adiabatic planar flame [25]) and heat is conducted toward the wall since the burned gas temperature is higher than that of the wall. However, at a relatively high stretch rate of $k = 1.0$, the flame is very close to the wall ($x_f = 0.54$). For this case, the maximum temperature in the burned gas region is lower than the wall temperature and thereby the flame is supported by heat feeding from the hot wall. At a high stretch rate, the flow residence time is short and the radical cannot be completely consumed by the recombination reaction. Therefore, the radical is accumulated in the burned zone as shown in Figure 3. Since the chemical enthalpy stored in the radical fails to be converted into thermal energy, Figure 3 shows that the temperature of the burned gas for the case of $k = 1.0$ is much lower than that for the case of $k = 0.1$. These observations are

qualitatively consistent with those results of wall stabilised methane-air flames with detailed mechanism [17].

To examine the effects of fuel Lewis number on flame-wall interaction, we plot the results for $Le_F = 0.5$ and $Le_F = 2.0$ in Figures 4(a) and 4(b), respectively. The results for the case of adiabatic wall (dashed lines) are also presented for comparison. The radical Lewis number is still fixed to be unity ($Le_Z = 1.0$). For $Le_F = 0.5$, Figure 4(a) indicates that the influence of the wall temperature T_w on the evolution of the x_f-k curve is qualitatively similar to that for unity fuel Lewis number shown in Figure 2. However, for $Le_F = 2.0$, new flame bifurcation appears when T_w is around unity, and the x_f -k curve becomes Z-shaped with two turning points (denoted by b and c). In Figure 4(b), points b and c divide the solutions for $T_w = 1.0$ and 1.02 into three regimes: the upper normal flame branch (ab), the middle unstable branch (bc), and the lower weak flame branch (cd). A similar phenomenon was also observed by Ju and Minaev [12] and Nakamura *et al.* [17]. Along the normal flame branch ab, the flame gradually approaches the wall as the stretch rate increases. At point b, it jumps to the weak flame branch cd for the case of $T_w = 1.02$ in Figure 4(b). On the cd branch, the flame is stabilised by heat conduction from the wall. However, for $T_w = 1.0$, the flame extinguishes at point b. For weak flames of $T_w = 1.02$ and 1.0, x_f increases with decreased k and jumps to the normal flame branch ab at turning point c. For $T_w \geq 1.1$, the premixed stagnation flame approaches the hot wall consecutively as the stretch rate increases and no flame extinguish occurs. For the case of adiabatic wall (dashed lines), the premixed flame bifurcates at the mere turning points and larger extinction stretch rates are observed compared to flames stabilised by a wall with fixed temperature. Therefore, according to results shown in Figures 2 and 4, the influence of wall temperature on the premixed stagnation flame is also affected by the fuel Lewis number. In Figures 2 and 4, the radical Lewis number is fixed to be unity. The effects of radical Lewis number on flame bifurcation and extinction are also studied (not shown in this paper). Unlike the fuel

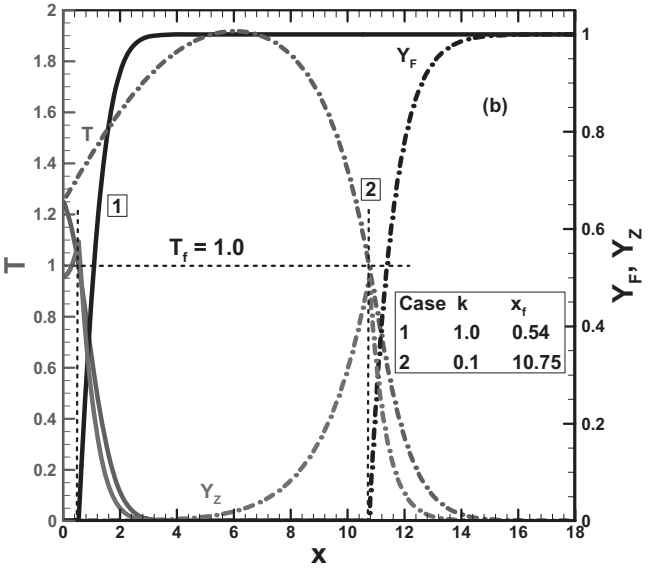

Figure 3. The temperature and fuel and radical mass fraction distributions for $T_w = 1.25$ and $Le_F = Le_Z = 1$.

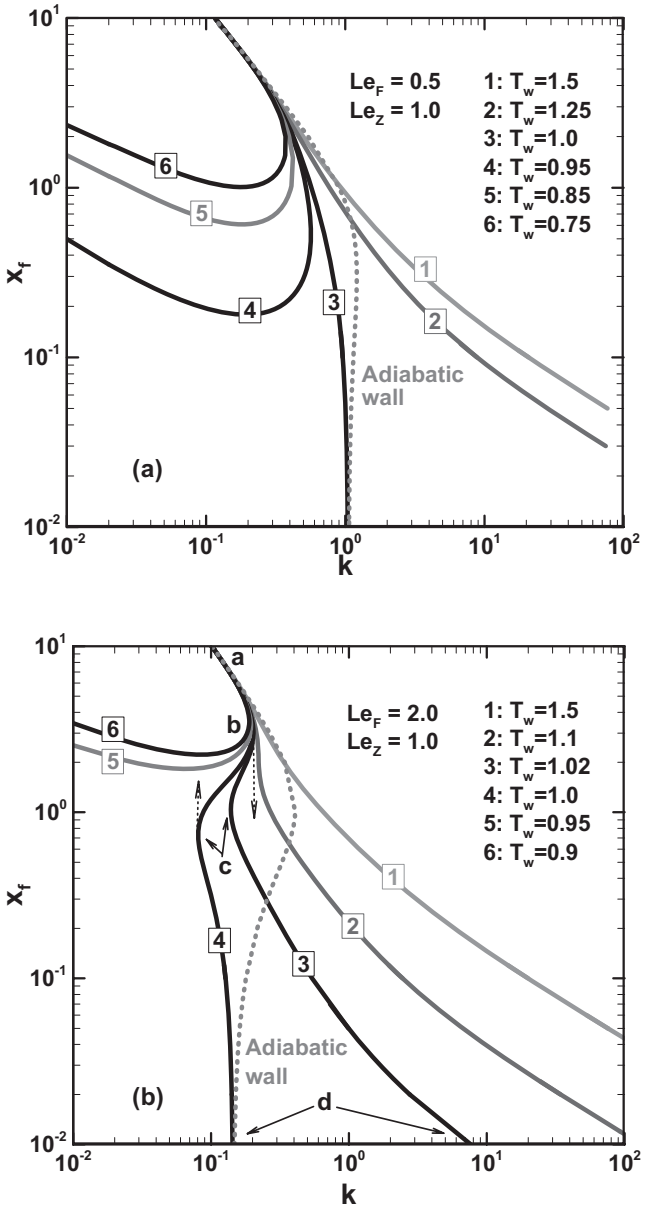

Figure 4. Flame position as a function of stretch rate for (a) $Le_F = 0.5$ and (b) $Le_F = 2.0$.

Lewis number, the radical Lewis number only has a quantitative influence on the flame-wall interaction and no qualitative change is observed.

In order to compare the weak and normal flames observed in Figure 4(b), their flame structures are plotted in Figure 5. The wall temperature T_w is unity and the stretch rate k is 0.11. It is seen that the temperature and radical mass fraction of the normal flame are much higher than these of the weak flame. The peak temperature T_{max} in the burned zone of the weak flame is very close to the cross-over temperature $T_c = 1$, indicating that there is

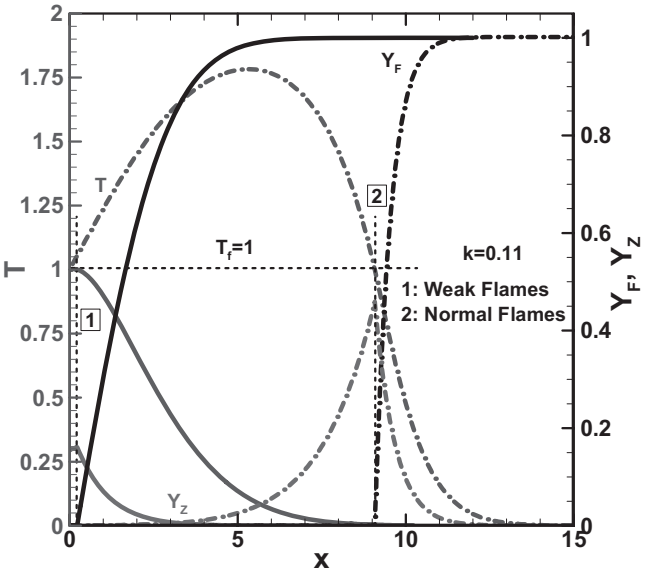

Figure 5. Flame structures for normal and weak flames with stretch rate $k = 0.11$ for $Le_F = 2$ and $Le_Z = 1$.

negligible heat release from the chemical reaction. These are qualitatively similar to the comparison between the structures of normal and weak flames obtained from simulation considering detailed chemistry [17]. Moreover, it is interesting to compare the weak flame in Figure 5 with the normal flame very close to the wall shown as Case 1 in Figure 3. It is observed that the weak flame has much lower radical concentration and a negligible temperature increment in the post flame region. This can be justified by the fact that in the present framework of chemical kinetics, both chain-branching and recombination reactions proceed at a small rate in the weak flame regime. However, for the flame very close to the wall ($x_f = 0.54$) shown in Figure 3, the recombination reaction cannot consume the radical due to the short flow residence time. Therefore, although both aforementioned flames are very close to the wall, nevertheless, their structures and underlying chemistry response are quite different.

Figure 6 demonstrates the effects of the fuel and radical Lewis numbers on the extinction stretch for the cases of $T_w = 0.7$ (solid lines) and adiabatic wall (dashed lines). It is seen that k_{ext} monotonically increases (decreases) with Le_Z (Le_F). This is due to the coupling between the preferential thermal-mass diffusion and positive stretch rate. The fuel diffuses into the reaction zone, and the positively stretched stagnation flame becomes weaker and thereby is more easily extinguished when the fuel Lewis number becomes larger [37, 39, 41, 42]. Unlike the fuel, the radical diffuses out of the reaction zone. With the increase of the radical Lewis number (i.e. decease of the radical diffusivity), less radical enthalpy is diffused away from the reaction zone and hence the flame becomes stronger and more difficult to extinguish. A similar observation was found in our studies on positively stretched spherical flames [26–28]. Figure 6 also shows that the extinction stretch rate for the case of the adiabatic wall is higher than these for $T_w = 0.7$. This can be justified by the fact that the existence of the wall with $T_w = 0.7$ weakens the flame so that the flame cannot be reactive in a relatively large stretch rate. Furthermore, Figure 6(b) indicates that the change

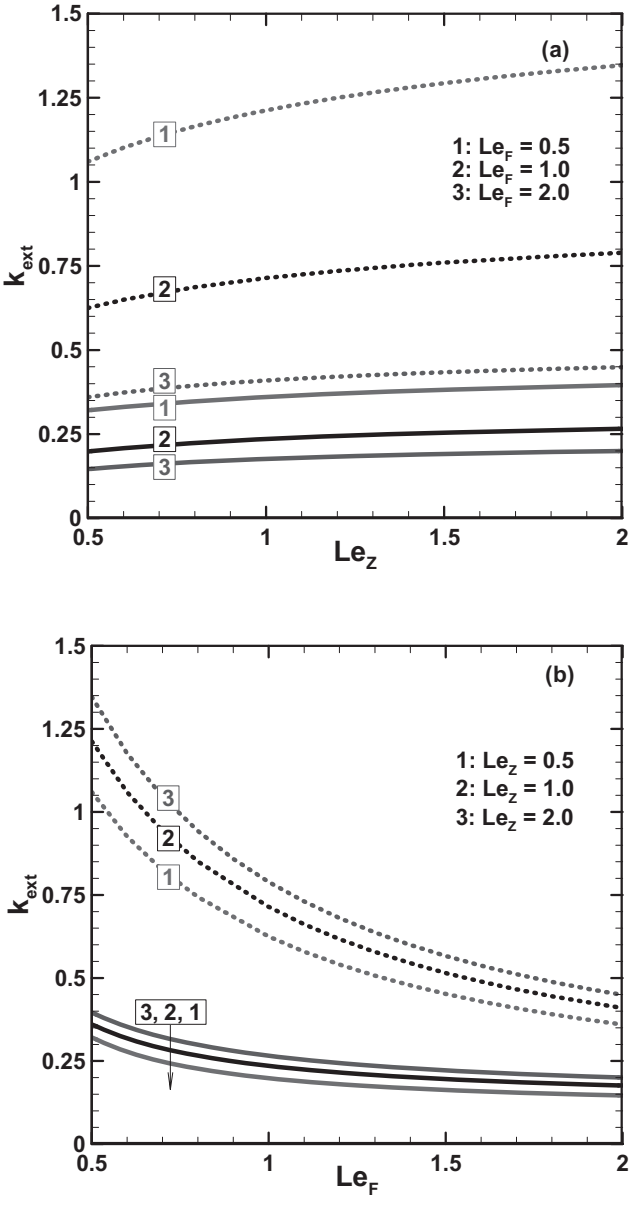

Figure 6. Dependence of the extinction stretch rate on (a) Le_Z and (b) Le_F. The dashed lines are the results from the premixed stagnation flame with the adiabatic wall, while the solid ones are from the premixed stagnation flame with $T_w = 0.7$.

of the extinction stretch rate with the fuel Lewis number is much larger for the case of the adiabatic wall than that for $T_w = 0.7$. This observation explicitly indicates that the non-adiabatic wall weakens the preferential diffusion effect which is expected to considerably influence the stretched flame [41]. Therefore, the existence of the wall has a great influence on the extinction stretch rate of premixed stagnation flames.

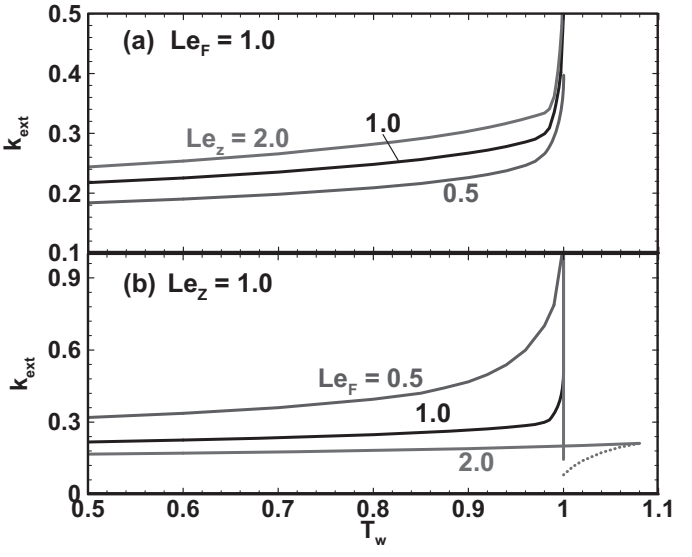

Figure 7. Dependence of the extinction stretch rate on the wall temperature.

Figure 7 demonstrates the effects of wall temperature T_w on the extinction stretch rate k_{ext} at different fuel and radical Lewis numbers. The extinction stretch rate k_{ext} is shown to increase monotonically with the wall temperature T_w. As shown in Figures 2 and 4, when the wall temperature is above the cross-over temperature, there is no flame extinguishment. Consequently, the extinction stretch rate increases exponentially when the wall temperature is close to unity. At $Le_F = 2.0$ shown in Figure 7(b), the extinction stretch rate k_{ext} for $T_w = 1$ is the stretch rate when the flame touches the wall and the extinction stretch rate k_{ext} for $T_w > 1$ physically corresponds to the value at which the normal flame becomes a weak flame (from the *ab* branch to *cd* branch in Figure 4(b)). Besides, for $Le_F = 2.0$ the minimum stretch rate below which the weak flame regime cannot exist is also plotted in Figure 7(b) and corresponds to the point *c* in Figure 4(b). It can be found from Figure 7(b) that the point *c* appears around $T_w = 1$, and increases with T_w. The turning points *b* and *c* merge around $T_w = 1.08$. Nevertheless, no extinction stretch rate exists when the wall temperature is above the cross-over temperature.

The above analysis shows that the wall temperature has great impact on flame bifurcations and extinction. To understand the heat transfer between the flame and wall, the temperature distributions for flames close to ($x_f = 1.0$) and far from ($x_f = 10.0$) the wall are presented in Figure 8. It is observed that the wall temperature has a pronounced effect on the temperature in both burned and unburned regions for near-wall premixed flames ($x_f = 1.0$). With the decrease of wall temperature, great change in the wall heat conduction (i.e. the temperature gradient at $x_f = 0$ in Figure 8) is observed. The gas is heated and cooled by the wall for $T_w > 1.25$ and $T_w \leq 1.25$, respectively. Furthermore, the magnitude of temperature gradient at the flame sheet, $x_f = 1.0$, becomes small with the decrease of the wall temperature, indicating that the heat transfer at the flame front is also greatly influenced by the wall temperature. When the flame front is far from the wall ($x_f = 10$), the temperature distribution around the flame front is not affected by the wall temperature. Therefore, the effects of wall temperature and heat flux on the flame front are negligible when the flame sheet is far away from the wall.

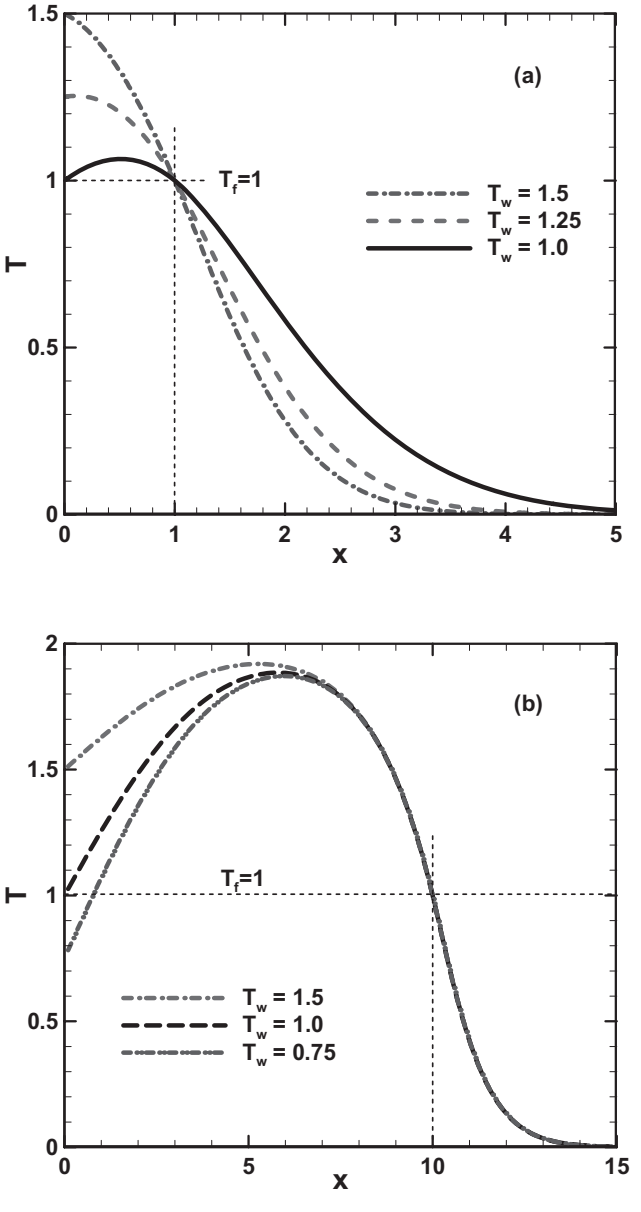

Figure 8. Temperature distributions at different wall temperatures with unity Lewis numbers of fuel and radical for (a) $x_f = 1.0$ and (b) $x_f = 10.0$.

In order to further quantify the heat transfer at the wall ($x = 0$) and the flame front ($x = x_f$), the corresponding normalised heat fluxes, q_w and q_f, can be readily obtained based on Equation (16)

$$q_w = -\frac{dT}{dx}\bigg|_{x=0} = \left[T_w - 1 - \int_0^{x_f}\int_0^{\eta} I(\varsigma,\eta)d\varsigma d\eta\right] \Big/ \int_0^{x_f} e^{-\frac{1}{2}\varsigma^2 k} d\varsigma \tag{19a}$$

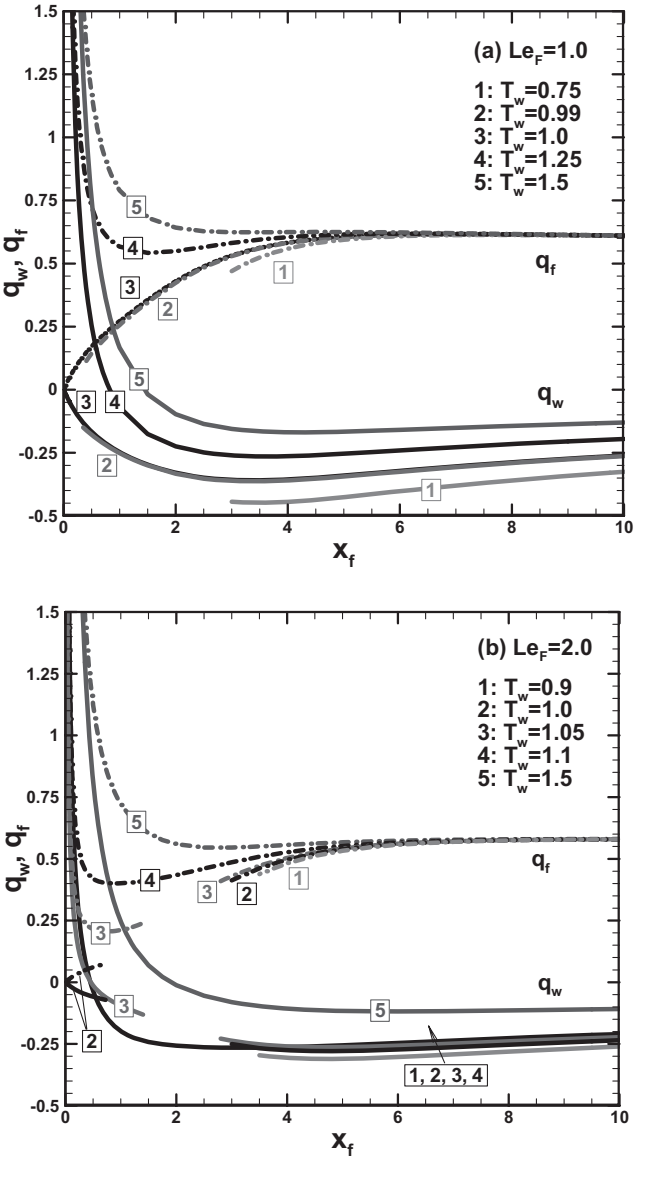

Figure 9. Change of the heat fluxes at the wall and the flame front with the flame position at different wall temperatures for (a) $Le_F = 1$ and (b) $Le_F = 2$.

$$q_f = -\left.\frac{dT}{dx}\right|_{x=x_f} = \left[T_w - 1 + \int_0^{x_f}\int_\eta^{x_f} I(\varsigma,\eta)d\varsigma d\eta\right] \Big/ \int_0^{x_f} e^{-\frac{1}{2}(\varsigma^2 - x_f^2)k} d\varsigma \qquad (19b)$$

When $q_w > 0$, the heat is fed to the gaseous mixture from the wall; while the heat is conducted to the wall when $q_w < 0$. q_f is always positive due to the release of chemical enthalpy near the flame front. It is noted that in the present investigation only the radical loss on the wall (i.e. the third equality in Equation (7a)) is considered and it is energetically

neutral. If the radical quenching reaction and hence its heat release are taken into account, an additional correction term would appear in Equations (1c) and (5c) and hence (19a). However, the heat release from the wall radical reaction may be small compared to that from the reaction sheet when the flame is not very close to the wall and/or the wall temperature is high. Thus it is expected to have a negligible influence on the wall heat flux shown in Equation (19a). For those cases in which the distance between the flame and wall is very small and/or the wall temperature is relatively high, the heat release from the wall radical reaction may show some extent of influence, which may be discussed in a future paper.

Based on Equation (19a), the non-dimensional heat flux at the wall ($x_f = 0$), q_w, is plotted as a function of flame position x_f at different wall temperatures in Figure 9 (solid lines). The radical Lewis number is fixed to be unity and only the results of the stable flame branches (e.g. branch *ab* in Figure 4(b)) are given in Figure 9. When $Le_F = 1$ shown in Figure 9(a), for $T_w = 1.25$ and $T_w = 1.5$, wall heat flux q_w is first positive (i.e. the heat is conducted away from the wall and thus the gas is heated by the wall) and then becomes negative (i.e. the heat is conducted toward the wall and thus the gas is cooled by the wall) with the increases of the separation distance between the flame and wall. This is due to the change in the temperature distribution with the flame position, as shown in Figure 8. Furthermore, Figure 9(a) shows that, when $q_w < 0$, $|q_w|$ first increases and then approaches zero as the flame position x_f gradually increases. This is due to the fact that the wall heat flux depends on the flame position as well as the maximum temperature (which increases with the flame position). According to the results not shown in Figure 9(a), when x_f is large enough, the wall heat flux q_w is close to zero, indicating that there is no thermal interaction between flame and wall. When $T_w \leq 1$, wall surfaces always cool the burned gas near the wall ($q_w \leq 0$). The results for $Le_F = 2.0$ shown in Figure 9(b) are similar to those for $Le_F = 1.0$ in Figure 9(a). The primary difference is the discontinuity of q_w due to the existence of physically unstable solutions (i.e. *bc* branch in Figure 4(b)).

Based on Equation (19b), the heat flux at the flame front is also given in Figure 9 (dash-dotted lines) to demonstrate the influence of wall temperature on the heat transfer at the flame front. For $Le_F = 1$, Figure 9(a) shows that the heat flux at the flame front q_f monotonically increases with x_f for $T_w \leq 1$ while it decreases for $T_w > 1$. The former behaviours again corroborate the flame quenching caused by the stretch $T_w \leq 1$. Also, for $T_w > 1$, q_w and q_f share the same large values, and this further confirms the conclusions from Figure 2 that the flame always exists for $T_w > 1$. What is more, from Figure 9(a), it can be found that when $x_f > 6$, q_f approaches a constant value 0.6, indicating that when the flame stabilisation position is beyond 6, the wall temperature influence is negligible. For $Le_F = 2.0$, similar dependence of heat flux at normal flame fronts is observed in Figure 9(b). However, the heat flux at weak flame fronts shows different behaviours with different T_w in Figure 9(b): for $T_w = 1$, q_f decreases and ultimately equals zero (extinction occurs) with decreased flame position x_f; for $T_w = 1.25$, as x_f decreases, q_f first decreases and then increases to a large value. Therefore, although both cases mentioned above are weak flames, the heat transfer at their flame fronts considerably differs due to influence of the wall temperature. Here it should be emphasised that, based on the curves corresponding to $T_w = T_c = 1$ in Figures 9(a) and 9(b), q_f approaches zero when the flame is located at $x_f = 0$. This is due to the fact that the chain-branching reaction is assumed to be infinitely fast once the local temperature reaches the cross-over temperature. In fact, if the finite rate of the chain-branching reaction (i.e. the structure of the radical production zone) is taken into consideration, the conclusion about q_f when the flame is very close to the wall will be corrected.

The wall heat flux as a function of the wall temperature is plotted in Figure 10 for different stretch rates or Lewis numbers. It is seen that the wall heat flux q_w increases almost linearly with the wall temperature T_w. The same trend was also observed in previous numerical [1, 14] and experimental [43] studies. Figure 10(a) shows that the stagnation flame can always exist for different stretch rates when $T_w > 1$. However, for $k = 0.5$, 1 and 5, there is no flame when $T_w < 1$. Figure 10(a) also shows that at small stretch rates ($k =$ 0.15 and 0.5), q_w is always negative indicating that heat is conducted towards the wall from the burned gas. At large stretch rates ($k = 1$ and 5), q_w becomes positive and the extent to which the wall heats the gas increases with increased stretch rate. Figure 10(b) indicates that the wall heat flux increases/decreases with the fuel/radical Lewis number. This is due to the fact that the positively stretched stagnation flame is affected in opposite manners by the fuel and radical Lewis numbers as mentioned before. Moreover, Figure 10(b) shows that the radical Lewis number has much weaker influence on the wall heat flux than the fuel Lewis number. This is consistent with the conclusion that the positively stretched flame is much more strongly affected by the fuel Lewis number than by the radical Lewis number [26–28].

In a brief summary, the above results show even when there is no radical quenching on the wall, the premixed stagnation flame is strongly affected by the wall temperature in terms of flame bifurcations and extinction. The extinction stretch rate increases with fuel Lewis number as well as the wall temperature and it decreases with the radical Lewis number. Furthermore, the heat fluxes at the wall and flame front are found to be greatly affected by the wall temperature when the separation distance between the wall and flame is small. The wall heat flux is shown to change almost linearly with the wall temperature.

4.2. *Effects of radical quenching on the wall*

In this subsection the radical quenching on the wall surface is considered and the radical quenching coefficient r_q is negative. Figure 11 shows the results at different radical quenching coefficients. The wall temperature T_w is kept to be 1.0. In Figure 11(a) with $Le_F = Le_Z = 1$, when there is no radical quenching on the wall (i.e. $r_q = 0$), the flame position x_f decreases monotonically with the stretch rate k. However, when radical quenching on the wall is considered ($r_q < 0$), the x_f-k curve becomes reverse C-shaped and flame extinction occurs at the turning point. At a large stretch rate and thereby small separation distance between the flame and wall, the flame is extinguished by the radical quenching on the wall surface. Figure 11(b) presents the results for $Le_F = 2$ and $Le_Z = 1$. As shown in Figure 4(b), the x_f-k curve for $r_q = 0$ is Z-shaped with two turning points. Flame extinction occurs at the right turning point *b*. At a small magnitude of the radical quenching coefficient (i.e. $r_q = -0.5$), the Z-shaped curve is shifted towards the left. With relatively strong radical quenching on the wall surface (i.e. $r_q =$ -1.0, -5.0, and -10.0), the x_f-k curve becomes reverse C-shaped and the near-wall flame cannot appear due to the radical quenching. In both Figures 11(a) and 11(b), the x_f-k curves corresponding to the negative infinite value of radical quenching coefficients (i.e. $r_q \to -\infty$) are demonstrated. It can be seen that in this limit case, these curves are reverse C-shaped and when $|r_q| > 5.0$, the x_f-k curves are very close to those of the limit case. This means that when $|r_q| > 5.0$, the radical destruction due to the wall has a minor influence on the relation between the flame position and the stretch rate.

Figure 12 shows the extinction stretch rates k_{ext} as a function of the radical quenching coefficient r_q. The solid curve corresponds to extinction at the turning point (point *b* in Figure 11(b)). The open circle represents the critical state at which the turning point on

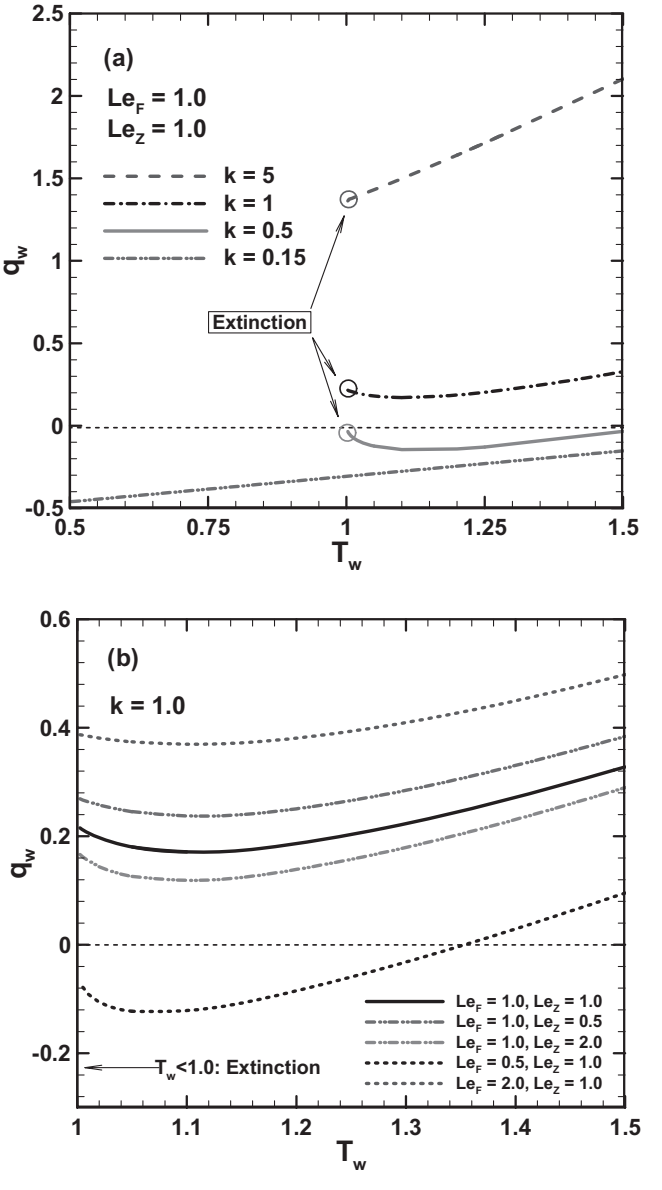

Figure 10. The wall heat flux as a function of wall temperature for different (a) stretch rates and (b) Lewis numbers.

x_f-k curve appears (see Figure 11(a)). The corresponding radical quenching coefficient at this critical state is denoted as $r_{q,c}$. For $Le_F = 0.5$ and 1.0, the flame extinguishes at the turning point with $|r_q| \geq |r_{q,c}|$ (see Figure 11). As expected, the extinction stretch rate k_{ext} is shown to decrease with the magnitude of the radical quenching coefficient $|r_q|$. It is noted that for $Le_F = 2.0$, the turning point always exists (see Figure 11(b)) in Figure 12(a). Also, for $Le_F = 2.0$ the minimum stretch rate for weak flame regime (i.e. point c in Figure 11(b)) is also shown in Figure 12(a) (i.e. the dash-dotted line 3c). As $|r_q|$ increases, this minimum

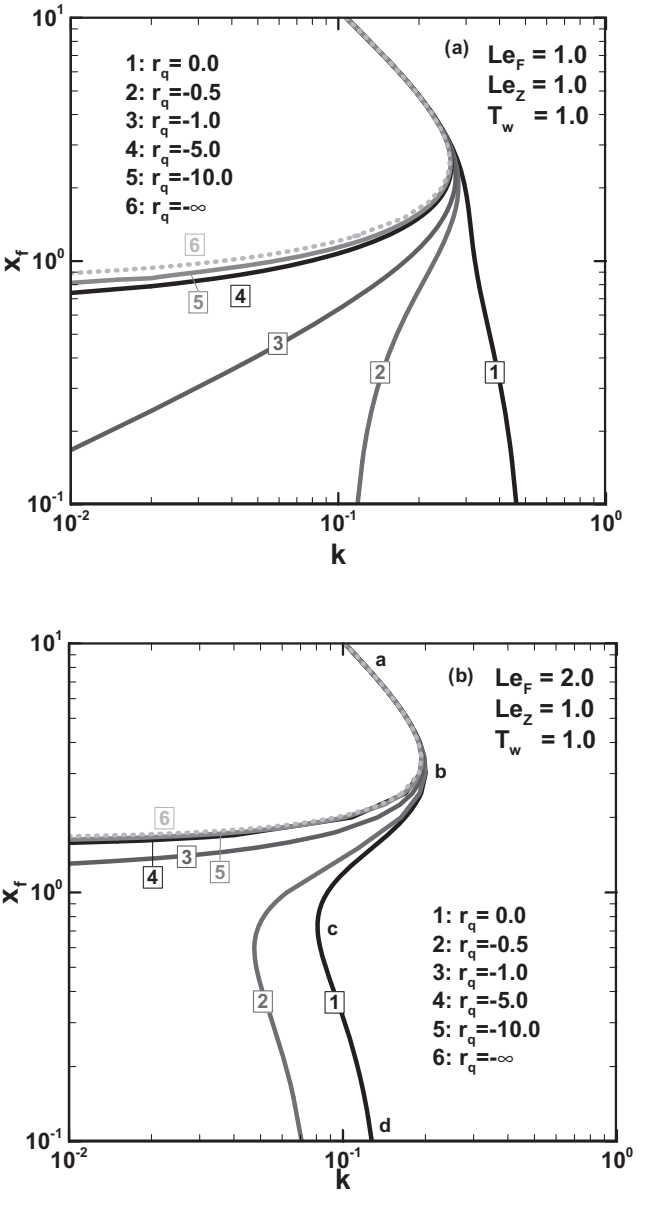

Figure 11. Flame position as a function of flame stretch rate for different radical quenching coefficients with (a) $Le_F = 1$ and (b) $Le_F = 2$.

stretch rate decreases and is always smaller than the extinction stretch rate corresponding to point *b*. Furthermore, Figure 12 indicates that effects of radical quenching on the extinction stretch rate are influenced by the Lewis numbers of fuel and radical.

To assess the wall temperature influence on radical quenching on the wall, flame position as a function of flame stretch for $T_w = 0.85$ and 1.25 is plotted in Figure 13. For $T_w = 0.85$, Figure 13(a) shows that the x_f -k curve is reverse *C*-shaped. The extinction stretch rate at the turning point slightly decreases as the magnitude of the radical quenching coefficient

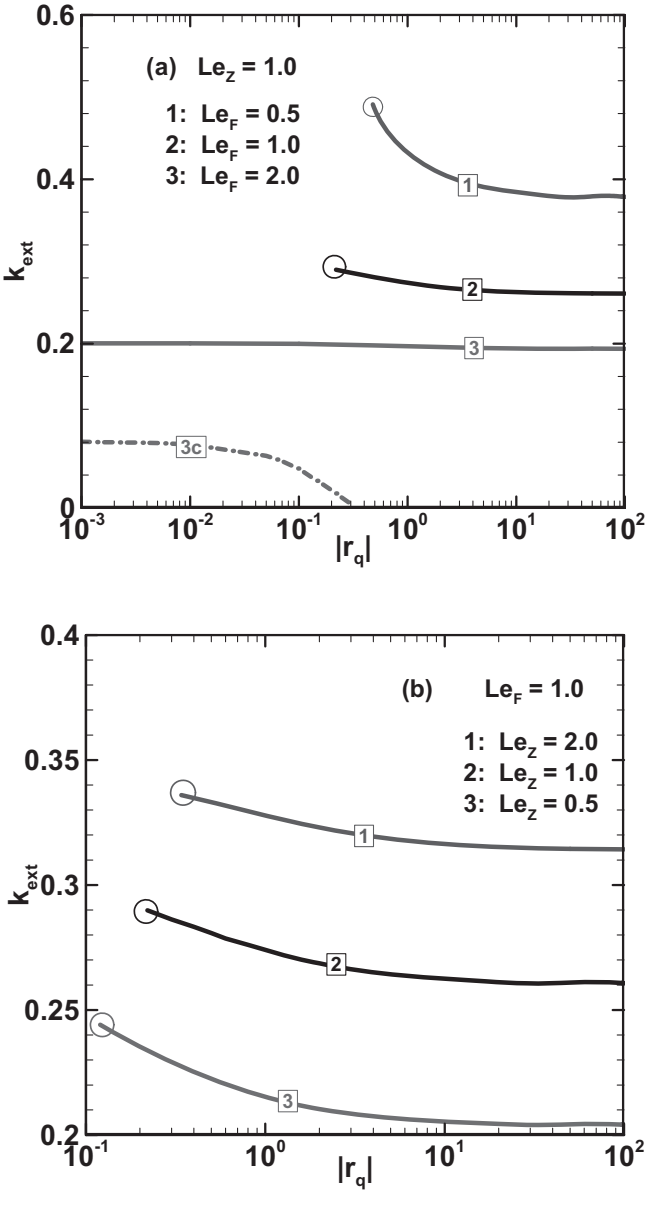

Figure 12. Extinction stretch rate as a function of the radical quenching coefficient with different (a) fuel and (b) radical Lewis numbers.

$|r_q|$ increases. The flame extinction occurs at $x_f = 2.5$ and thereby the radical quenching on the wall has weak influence on the extinction stretch rate. In Figure 13(b) with $T_w = 1.25$, the effect of radical quenching on flame position becomes negligible when $x_f < 0.07$ or $x_f > 4.0$. For small x_f (i.e. $x_f < 0.07$), radicals are easily transported to and quenched on the wall surface. However, for $T_w = 1.25$ in Figure 13(b), the wall temperature is larger than the flame front temperature. Accordingly, heat is always fed to the flame from the hot wall, and this offsets the weakening effect caused by radical quenching on the wall. Thus the

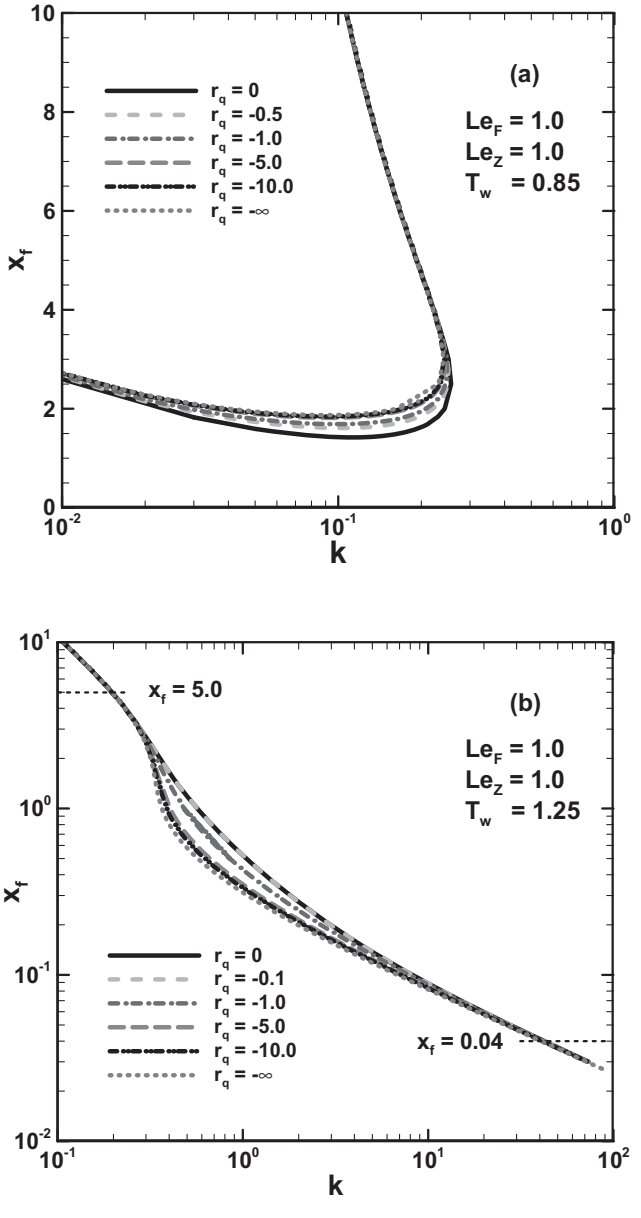

Figure 13. Flame position as a function of flame stretch rate for different radical quenching parameters with (a) $T_w = 0.85$ and (b) $T_w = 1.25$.

combined effects discussed above lead to the fact that the radical quenching has no obvious influence on the premixed flame on the wall with $T_w = 1.25$ as shown in Figure 13(b). Similar to Figures 11(a) and 11(b), the flame position as a function of flame stretch for $r_q \to -\infty$ is shown in Figures 13(a) and 13(b). Obviously, when $r_q < 5.0$, the x_f-k curves are very close to those for $r_q \to -\infty$.

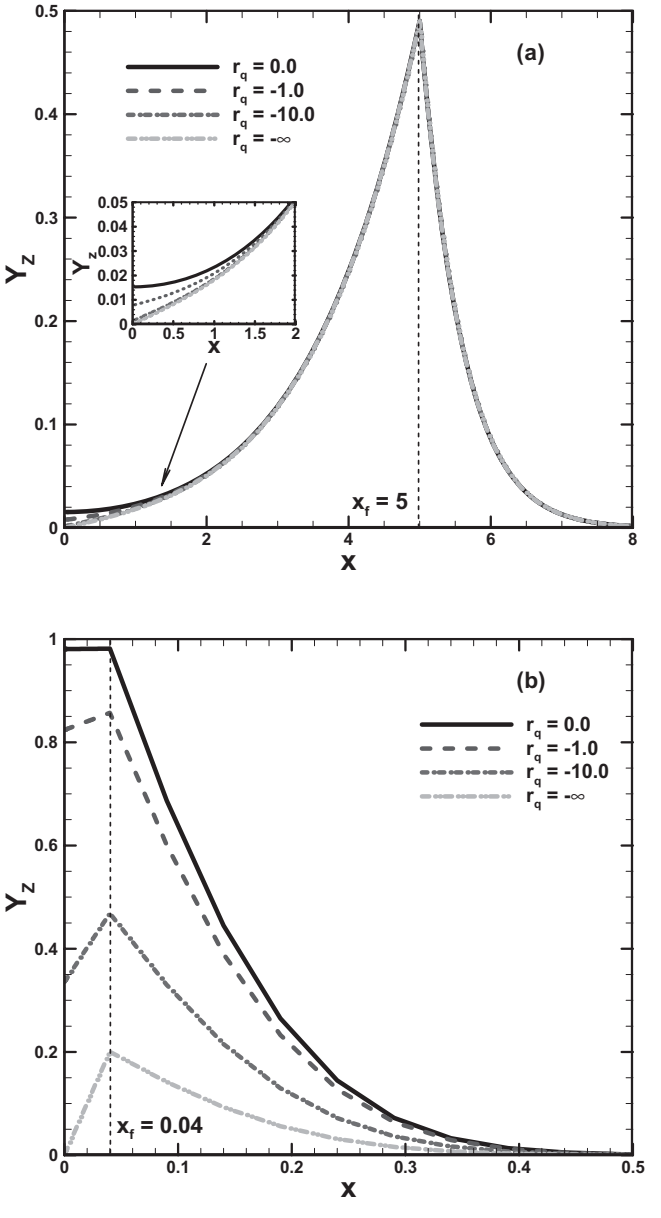

Figure 14. Distributions of radical mass fractions for different radical quenching coefficients with Lewis number $Le_F = Le_Z = 1.0$ and wall temperature $T_w = 1.25$. The flame positions are (a) $x_f = 5.0$ and (b) $x_f = 0.04$, respectively.

Although the radical quenching has negligible influence on relatively large and small flame positions shown in Figure 13(b), it does affect the radical mass fraction profile as shown in Figure 14. When the flame is far away from the wall ($x_f = 5.0$), it is observed that the radical quenching coefficient r_q has only marginal influence on radical mass fraction Y_Z for $0 < x < 2.0$ (see the inset of Figure 14(a)). For $x > 2.0$, the radical mass fractions

show no distinctions with different radical quenching coefficients. Even for $r_q \to -\infty$, the radical mass fraction was not considerably influenced by the wall radical destruction. When the flame is close to the wall, Figure 14(b) shows that the radical mass fraction profile is greatly affected by the radical quenching. Specifically, as the magnitude of the radical quenching coefficient $|r_q|$ increases, the radical mass fraction Y_Z considerably decreases. When $r_q \to -\infty$, the radical mass fraction at the wall is zero, indicating that the complete radical depletion occurs in this limit situation. Furthermore, the radical mass fraction Y_Z at the flame front is relatively low compared to those corresponding to the finite values of radical quenching coefficients.

5. Conclusions

Flame-wall interaction is studied theoretically using the premixed stagnation flame stabilised by a wall and the simplified Zel'dovich-Liñán model [24, 25] in which thermally sensitive intermediate kinetics is considered. Asymptotic analysis is conducted within the framework of large activation energy and potential flow, and the relationship between the flame position and stretch rate is derived. Based on this relationship, the effects of wall heat conduction and radical quenching on stretched premixed stagnation flame are examined.

The wall temperature strongly affects the bifurcation and extinction of the stretched premixed flame near a wall. The extinction stretch rate increases with the radical Lewis number as well as the wall temperature and decreases with the fuel Lewis number. When the flame is close to the wall, the wall temperature greatly influences the temperature distribution and the heat fluxes at the wall surface and flame front. The premixed flame is quenched far from the wall by stretch rate when the wall temperature is below the cross-over temperature, while it does not extinguish when the wall temperature is above the cross-over temperature. The heat fluxes at the wall increases linearly with the wall temperature.

The radical quenching on the wall also has great influence on flame bifurcation and extinction only when the flame is close to the wall. When the magnitude of the radical quenching coefficient is smaller than a critical value, the premixed flame is quenched near the wall surface. However, the flame extinguishes at the turning point when the magnitude of the radical quenching coefficient is above some critical value. Furthermore, the coupling between the wall heat conduction and radical quenching greatly influences the bifurcation and extinction of the premixed stagnation flame near a wall. For wall temperature below the cross-over temperature, the stable flame positions barely change as the radical quenching coefficient varies. For wall temperature above the cross-over temperature, the stable flame is affected within intermediate flame positions. The radical mass fraction profiles are greatly influenced by radical quenching effects at the wall when the separation distance is small. The limit case for negative infinite radical quenching coefficients is also considered for comparison.

It is noted that the analysis is valid at the limit of infinitely large activation energy of chain-branching reaction and therefore the analysis is not general. We do not consider the finite-rate kinetics for the chain-branching reaction, for which other distinguished limits might appear. Furthermore, other factors such as thermal expansion and boundary layer are not taken into consideration in the present investigation. The thermal expansion may also affect the premixed flame when it is close to the hot wall and explicitly change the mass/heat transfer. Besides, when the gas impinges toward the wall, the boundary layers for flow, temperature, and mass concentration may affect the premixed flame. These simplifications can be overcome by simulations considering detailed chemistry, which will be part of future work.

Acknowledgments

This work was supported by National Natural Science Foundation of China (Nos. 51136005 and 50976003) and Doctoral Fund of Ministry of Education of China (Nos. 20120001110080 and 20100001120003).

References

[1] T. Poinsot and D. Veynante, *Theoretical and Numerical Combustion*, Edwards, Philadelphia, 2005.
[2] Y.G. Ju and K. Maruta, *Microscale combustion: Technology development and fundamental research*, Prog. Energy Combust. Sci. 37 (2011), pp. 669–715.
[3] N.S. Kaisare and D.G. Vlachos, *A review on microcombustion: Fundamentals, devices and applications*, Prog. Energy Combust. Sci. 38 (2012), pp. 321–359.
[4] K. Maruta, *Micro and mesoscale combustion*, Proc. Combust. Inst. 33 (2011), pp. 125–150.
[5] T.V. Karman and G. Millan, *Thermal theory of a laminar flame front near a cold wall*, Fourth Symposium (International) on Combustion, 1953.
[6] A.A. Adamczyk and G.A. Lavoie, *Laminar head-on flame quenching: A theoretical study*, SAE Trans. 87 (1978), SAE paper 780969, 1978.
[7] G.F. Carrier, F.W. Fendell, W.B. Bush, and P.S. Feldman, *Nonisenthalpic interaction of a planar premixed laminar flame with a parallel end wall*, SAE Paper 790245, 1979.
[8] C.K. Westbrook, A.A. Adamczyk, and G.A. Lavoie, *A numerical study of laminar flame wall quenching*, Combust. Flame. 40 (1981), pp. 81–99.
[9] W. Hocks, N. Peters, and G. Adomeit, *Flame quenching in front of a cold wall under two step kinetics*, Combust. Flame. 41 (1981), pp. 157–170.
[10] D.G. Vlachos, L.D. Schmidt, and R. Aris, *Ignition and extinction of flames near surfaces: Combustion of H_2 in air*, Combust. Flame. 95 (1993), pp. 313–335.
[11] F.N. Egolfopoulos, H. Zhang, and Z. Zhang, *Wall effects on the propagation and extinction of steady, strained, laminar premixed flames*, Combust. Flame. 109 (1997), pp. 237–252.
[12] Y.G. Ju and S. Minaev, *Dynamics and flammability limit of stretched premixed flames stabilized by a hot wall*, Proc. Combust. Inst. 29 (2002), pp. 949–956.
[13] H. Nakamura, A. Fan, S. Minaev, E. Sereshchenko, R. Fursenko, Y. Tsuboi, and K. Maruta, *Bifurcations and negative propagation speeds of methane/air premixed flames with repetitive extinction and ignition in a heated microchannel*, Combust. Flame. 159 (2012), pp. 1631–1643.
[14] P. Popp and M. Baum, *Analysis of wall heat fluxes, reaction mechanisms, and unburnt hydrocarbons during the head-on quenching of a laminar methane flame*, Combust. Flame. 108 (1997), pp. 327–348.
[15] C. Hasse, M. Bollig, N. Peters, and H.A. Dwyer, *Quenching of laminar iso-octane flames at cold walls*, Combust. Flame. 122 (2000), pp. 117–129.
[16] P. Popp, M. Smooke, and M. Baum, *Heterogeneous/homogeneous reaction and transport coupling during flame-wall interaction*, Twenty-Sixth Symposium (International) on Combustion, 2 (1996), pp. 2693–2700.
[17] H. Nakamura, A. Fan, H. Minamizono, K. Maruta, H. Kobayashi, and T. Niioka, *Bifurcations of stretched premixed flame stabilized by a hot wall*, Proc. Combust. Inst. 32 (2009), pp. 1367–1374.
[18] I.S. Wichman and G. Bruneaux, *Head-on quenching of a premixed flame by a cold wall*, Combust. Flame. 103 (1995), pp. 296–310.
[19] P. Aghalayam, P.A. Bui, and D.G. Vlachos, *The role of radical wall quenching in flame stability and wall heat flux: Hydrogen-air mixtures*, Combust. Theory Model. 2 (1998), pp. 515–530.
[20] M. Gummalla, P.-A. Bui, and D.G. Vlachos, *Nonlinear dynamics of surface stabilized premixed and dilusion flames: Current trends and future directions*, Chem. Eng. Sci. 55 (2000), pp. 311–319.
[21] P.A. Bui, D.G. Vlachos, and P.R. Westmoreland, *Modeling ignition of catalytic reactors with detailed surface kinetics and transport: Oxidation of H_2/air mixtures over platinum surfaces*, Ind. Eng. Chem. Res. 36 (1997), pp. 2558–2567.
[22] D.G. Vlachos, *The interplay of transport, kinetics, and thermal interactions in the stability of premixed hydrogen/air flames near surfaces*, Combust. Flame. 103 (1995), pp. 59–75.
[23] Y. Saikia and Y. Suzuki, *Effect of wall surface reaction on a methane-air premixed flame in narrow channels with different wall materials*, Proc. Combust. Inst. 34 (2013), pp. 3395–3402.

[24] J.W. Dold, R.W. Thatcher, A. Omon-Arancibia, and J. Redman, *From one-step to chain-branching premixed flame asymptotics*. Proc. Combust. Inst. 29 (2002), pp. 1519–1526.
[25] J.W. Dold, *Premixed flames modelled with thermally sensitive intermediate branching kinetics*, Combust. Theory Model. 11 (2007), pp. 909–948.
[26] H. Zhang and Z. Chen, *Spherical flame initiation and propagation with thermally sensitive intermediate kinetics*, Combust. Flame. 158 (2011), pp. 1520–1531.
[27] H. Zhang, P. Guo, and Z. Chen, *Critical condition for the ignition of reactant mixture by radical deposition*, Proc. Combust. Inst. 34 (2013), pp. 3267–3275.
[28] H. Zhang, P. Guo, and Z. Chen, *Outwardly propagating spherical flames with thermally sensitive intermediate kinetics and radiative loss*, Combust. Sci. Technol. 185 (2013) 226–248.
[29] V.N. Kurdyumov and D. Fernández-Galisteo, *Asymptotic structure of premixed flames for a simple chain-branching chemistry model with finite activation energy near the flammability limit*, Proc. Combust. Inst. 159 (2012), pp. 3110–3118.
[30] G.J. Sharpe, *Thermal-diffusion instability of premixed flames for a simple chain-branching chemistry model with finite activation energy*, SIAM J. Appl. Math. 70 (2009), pp. 866–884.
[31] V.V. Gubernov, H.S. Sidhu, and G.N. Mercer, *Combustion waves in a model with chain branching reaction and their stability*, Combust. Theory. Model. 12 (2008), pp. 407–431.
[32] V.V. Gubernov, H.S. Sidhu, and G.N. Mercer, *Combustion waves in a model with chain branching reaction*, J. Math. Chem. 39 (2006), pp. 1–14.
[33] V.V. Gubernov, A.V. Kolobov, A.A. Polezhaev, and H.S. Sidhu, *Oscillatory thermal-diffusive instability of combustion waves in a model with chain-branching reaction and heat loss*, Combust. Theory Model. 15 (2011), pp. 385–407.
[34] G.J. Sharpe and S.A.E.G. Falle, *Numerical simulations of premixed flame cellular instability for a simple chain-branching model*, Combust. Flame. 158 (2011), pp. 925–934.
[35] J.W. Dold, R.O. Weber, R.W. Thatcher, and A.A. Shah, *Flame balls with thermally sensitive intermediate kinetics*, Combust. Theory Model. 7 (2003), pp. 175–203.
[36] A. Liñán, *The asymptotic structure of counterflow diffusion flames for large activation energies*. Acta Astronaut. 1 (1974), pp. 1007–1039.
[37] Y. Ju, H. Guo, K. Maruta, and T. Niioka, *Flame bifurcations and flammable regions of radiative counterflow premixed flames with general Lewis numbers*, Combust. Flame. 113 (1998), pp. 603–614.
[38] Y. Ju, G. Masuya, F. Liu, H. Guo, K. Maruta, and T. Niioka, *Further examinations on extinction and bifurcations of radiative CH_4/air and C_3H_8/air premixed flames*, Proc. Combust. Inst. 27 (1998), pp. 2551–2557.
[39] Z. Chen, and Y. Ju, *Combined effects of curvature, radiation, and stretch on the extinction of premixed tubular flames*, Int. J. Heat Mass Transfer. 51 (2008), pp. 6118–6125.
[40] V.N. Kurdyumov, *Diffusive-thermal instability of premixed tubular flames*, Combust. Flame. 158 (2011), pp. 1718–1726.
[41] C.K. Law, *Combustion Physics*, Cambridge University Press, 2006.
[42] Z. Chen, X. Gou, and Y.G. Ju, *Studies on the outwardly and inwardly propagating spherical flames with radiative loss*, Combust. Sci. Technol. 182 (2010), pp. 124–142.
[43] L. Connelly, T. Ogasawara, D. Lee, R. Greif, and R.F. Sawyer, *Stagnation quenching of laminar, methane-air flames in a constant volume chamber: Wall temperature effects*, in Fall Meeting, volume WSCI 93-077. The Western States Section/The Combustion Institute, Stanford, CA, 1993.